Journal of Molecular Structure 1280 (2023) 135053

Contents lists available at ScienceDirect

Journal of Molecular Structure

journal homepage: www.elsevier.com/locate/molstr

Synthesis, characterization, in-vitro biological evaluation and theoretical studies of 1,2,3-triazoles derived from triclosan as difenoconazole analogues

Juana Suárez-García[a,b,c], Ma.-Angeles Cano-Herrera[a,b,c,*], Angela María-Gaviria[d], Víctor Manuel Osorio-Echeverri[d], Hugo Mendieta-Zerón[e], David Arias-Olivares[f], Julie Benavides-Melo[g], Luis Carlos García-Sánchez[h], Josue García-Ortíz[h], Andrés Becerra-Buitrago[h], Jessica Valero-Rojas[h], Mateo Rodríguez-González[h], Marco Antonio García-Eleno[a,b,c], Erick Cuevas-Yañez[a,b,c,*]

[a] Centro Conjunto de Investigación en Química Sustentable UAEM-UNAM, Carretera Toluca-Atlacomulco Km 14.5, Toluca, Estado de México, 50200, Mexico
[b] Universidad Autónoma del Estado de México
[c] Facultad de Química, Universidad Autónoma del Estado de México, Paseo Colon esq. Paseo Tollocan, Toluca, Estado de México, 50120, Mexico
[d] Grupo de investigación Biociencias, Facultad de Ciencias de la Salud, Institución Universitaria Colegio Mayor de Antioquia. Facultad de Ciencias de la Salud, Carrera 78 # 65-46, Medellín, Colombia
[e] Facultad de Medicina, Universidad Autónoma del Estado de México, Paseo Tollocan/Jesús Carranza s/n, Toluca, 50120, Mexico
[f] Center of Applied Nanoscience (CANS), Facultad de Ciencias Exactas, Universidad Andrés Bello, Avenida República 275, 8370146 Santiago, Chile
[g] Departamento de Química, Facultad de Ciencia y Tecnología, Universidad Pedagógica Nacional, Calle 72 No. 11 - 86, Bogotá, Bogotá, Colombia
[h] Grupo de Química Computacional y Sustentabilidad Ambiental, Universidad Distrital Francisco José de Caldas, Carrera 7 # 40B – 53, 11021-110231588 Bogotá, Colombia

ARTICLE INFO

Article history:
Received 5 August 2022
Revised 25 January 2023
Accepted 29 January 2023
Available online 30 January 2023

Keywords:
1,2,3-Triazole
Difenoconazole
Antimicrobial activity

ABSTRACT

An efficient synthesis of novel difenoconazole analogues is described. The synthetic route involves a Friedel-Crafts acylation on triclosan molecule followed by a sequential azide formation/CuAAC reaction in a single synthetic operation leading to 1-(2–chloro-5-(2,4-dichlorophenoxy)-4-hydroxyphenyl)-2-(4-(1-hydroxycyclohexyl)-1,2,3-triazol-1-yl)ethan-1-one derivatives in 50–96% yields. Synthesized 1,2,3-triazoles were evaluated for activity against diverse strains including bacterial strains of *Staphylococcus aureus* ATCC 29213, *Escherichia coli* ATCC 700891 and fungal strain *Candida albicans* ATCC 90028. A 1,2,3-triazole derivative bearing a $CH(OH)CH_3$ group displayed a selective activity against Methicillin-resistant *Staphylococcus aureus* (MRSA) comparable to Gentamicin standard. This selectivity can be attributed to a conformation adopted by 5–chloro-2-(2,4-dichloro-phenoxy)-phenol core enabling non-covalent interactions presenting a higher activity based on Fukui function on triazole ring.

1. Introduction

Azole antifungal group comprises a wide variety of molecules with an imidazole/1,2,4-triazole core which include a high diversity of functional groups used for modulating the well-known antimycotic properties found in these compounds [1,2]. From this group, Difenoconazole (molecule **1**, Scheme 1) is used as fungicide to control a wide range of diseases in crops playing a prominent role in pest control, in one of the few examples of clinically licensed triazoles used for this purpose [3].

Difenoconazole is a broad-spectrum fungicide with a recognized activity against cultures of *Acomycetes, Basidiomycetes* and *Deuteromycetes* [4,5], besides diverse species of the genus *Alternaria* [6–8], *Fusarium* [9], *Drechslera* [10], and *Gaeumannomyces* [11]. These properties provide a protective and curative effect against *Venturia inaequalis, Cercospora arachidicola* and *Alternaria solani* [12]. However, extensive use of difenoconazole has caused an increasing resistance to certain strains of *Aspergillus* [13–15], *Venturia* [16] and *Fusarium*, enabling the formation of mycotoxins as aflatoxins and deoxynivalenol which pollute and lessen the harvests [17]. Hence, development of more active difenoconazole analogues is highly desirable.

Difenoconazole antifungal activity is due in part to the appearance of heterocyclic ring but also to 2–chloro-4-(4-chlorophenoxy)-

* Corresponding authors: Universidad Autónoma del Estado de México
E-mail addresses: mdlacanoh001@profesor.uaemex.mx (M.-A. Cano-Herrera), ecuevasy@uaemex.mx (E. Cuevas-Yañez).

https://doi.org/10.1016/j.molstruc.2023.135053
0022-2860/

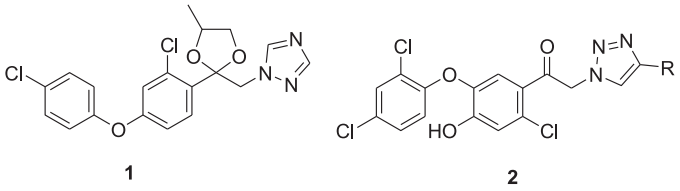

Scheme 1. Structure of Difenoconazole **1** and general structure for molecules **2** proposed in this work.

phenyl moiety present in Difenoconazole structure. This feature triggered our curiosity, and we hypothesized that new antimicrobial molecules might be obtained by gathering chloro phenoxy phenyl group and 1,2,3-triazole ring which, according to our experience [18,19], is easily available from CuAAC reaction through the Click Chemistry approach.

On this subject, CuAAC reaction has been thrivingly used for the preparation of new azole drugs libraries, emerging as a powerful synthetic tool through a strategy based on a heterocyclic ring change where imidazole/1,2,4-triazole is substituted by 1,2,3-triazole prepared from Click Chemistry obtaining derivatives with remarkable antifungal activity [20–26].

Concerning the 2–chloro-4-(4-chlorophenoxy)-phenyl counterparty in difenoconazole, a high similarity between this fragment and triclosan molecule is perceived. This compound is an antimicrobial agent broadly used in health care industry by virtue of its antimicrobial effectiveness and relatively harmlessness for humans [27,28]. These characteristics prompted us to consider the use of triclosan as a direct starting material in the design of a new sort of difenoconazole analogues.

With this idea in mind, we proposed the synthesis of a novel family of Difenoconazole analogues of type **2** (Scheme 1) with the purpose of exploring the inhibitory effect of these compounds on bacteria and fungi. Likewise, this paper discloses a theoretical study to determine a plausible explanation to antimicrobial activity found in these compounds. Recently, some authors agree in the importance of the DFT studies on this kind of molecules, where the Frontier Molecular Orbital (FMO) have been analyzed [29]. The FMO are directly related with the reactivity of this kind of compounds [30], and by other reactivity descriptors such as the here-employed Fukui's Function, or the extraction of non-covalent interactions, that in combination, gives and confirm the reaction mechanism of diverse molecules, and eventually related with the biological activity [31].

2. Experimental section

2.1. General remarks

The starting materials were purchased from Aldrich Chemical Co. and were used without further purification. Solvents were distilled before use. Silica plates of 0.20 mm thickness were used for thin layer chromatography. Melting points were determined with a Krüss Optronic melting point apparatus and they are uncorrected. ^{1}H and ^{13}C NMR spectra were recorded using a Bruker AVANCE 300; the chemical shifts (δ) are given in ppm relative to TMS as internal standard (0.00). For analytical purposes the mass spectra were recorded on a Shimadzu GCMS-QP2010 Plus in the EI mode, 70 eV, 200 °C via direct inlet probe. Only the molecular and parent ions (m/z) are reported. IR spectra were recorded on a Bruker TENSOR 27 FT instrument.

2.2. Synthesis of 2–chloro-1-(2–chloro-5-(2,4-dichlorophenoxy)–4 hydroxyphenyl)ethan-1-one (3)

To a stirred solution of chloroacetyl chloride (0.112 g, 2 mmol) in CH_2Cl_2 (3 mL) at 0 °C was added aluminum chloride (0.263 g, 2 mmol) portion wise for 15 min. The resulting mixture was stirred for 30 min at 0 °C. Triclosan (0.288 g, 1 mmol) was added portion wise for 15 min. The reaction mixture was stirred for 12 h at 65 °C. The dark blue solution was cooled at room temperature and carefully quenched with 3 mL of 30% HCl. The product was extracted with CH_2Cl_2 (3 × 5 mL), the organic layers were joined, washed with a saturated $NaHCO_3$ solution of and brine and dried over Na_2SO_4 and the solvent was removed under reduced pressure. Purification by flash chromatography (SiO_2, hexane/AcOEt 8:2) afforded 2–chloro-1-(2–chloro-5-(2,4-dichlorophenoxy)–4 hydroxyphenyl)ethan-1-one **3** as a pale yellow solid (0.218 g, 60%).

2.3. General procedure for the synthesis of 1,2,3-triazolyl difenoconazole analogues

Sodium azide (0.097 g, 1.5 mmol) was added to a stirred solution of 2–chloro-1-(2–chloro-5-(2,4-dichlorophenoxy)–4 hydroxyphenyl)ethan-1-one **3** (0.364 g, 1 mmol) in a 2:1 solution tBuOH–H_2O (5 mL) and the resulting mixture was stirred for 5 h at 65 ° The appropriate alkyne (1 mmol) was added followed by $CuSO_4{\cdot}5H_2O$ (0.012 g, 0.05 mmol) and a solution of L-ascorbic acid (0.044 g, 0.25 mmol) and $NaHCO_3$ (0.021 g, 0.25 mmol) in H_2O (1.2 mL). The resulting mixture was stirred at room temperature overnight. AcOEt (10 mL) was added, and the mixture was stirred for additional 30 min. The mixture was filtered through celite, and the product was extracted with ethyl acetate (3 × 5 mL). The organic layers were joined and dried over Na_2SO_4, and the solvent was removed under reduced pressure to afford the corresponding 1,2,3-triazolyl Difenoconazole analogues which was purified by flash column chromatography (SiO_2, hexane/AcOEt 8:2). Compounds **4–17** are represented in Scheme 2 and typical spectroscopic data are shown in Table 1.

2.4. In vitro antimicrobial activity

The antimicrobial activity of compounds **4–17** was screened following the standard procedure recommended by CLSI diffusimetric method [32].

2.4.1. Antimicrobial agents

A stock solution of Gentamicin (8 mg/ml) was used as a positive control for bacteria, whereas a solution of Fluconazole (5 mg/ml) was used as a positive control for yeasts, and Cycloheximide solution (5 mg/ml) was used for filamentous fungi. DMSO discs (10 μl) were used as negative control.

2.4.2. Media

The bacteria were slanted on Nutrient LB agar (Miller), yeasts were slanted on 4% Sabouraud dextrose agar (Merck), and the fungi were slanted on potato dextrose agar (Merck). Muller Hinton agar (MHA) were purchased from Sigma-Aldrich Co. and were used following the manufacturer's instructions for the antimicrobial assay.

2.4.3. Isolates

The following common pathogenic microorganisms were evaluated: standard strains of *Escherichia coli* ATCC 700891, *Staphylococcus aureus* ATCC 29213 and *Candida albicans* ATCC 90028, as well as a Gram-negative organism isolate of *Pseudomonas aeruginosa*; two Gram-positive isolates, namely, *Bacillus subtilis*, and methicillin-resistant *Staphylococcus aureus* (MRSA); and two fungal isolates, *Aspergillus niger* and *Fusarium sp*. and C. albicans. All the isolates were obtained from the Maternal Perinatal Hospital Monica Pretelini Sáenz, Toluca, Mexico.

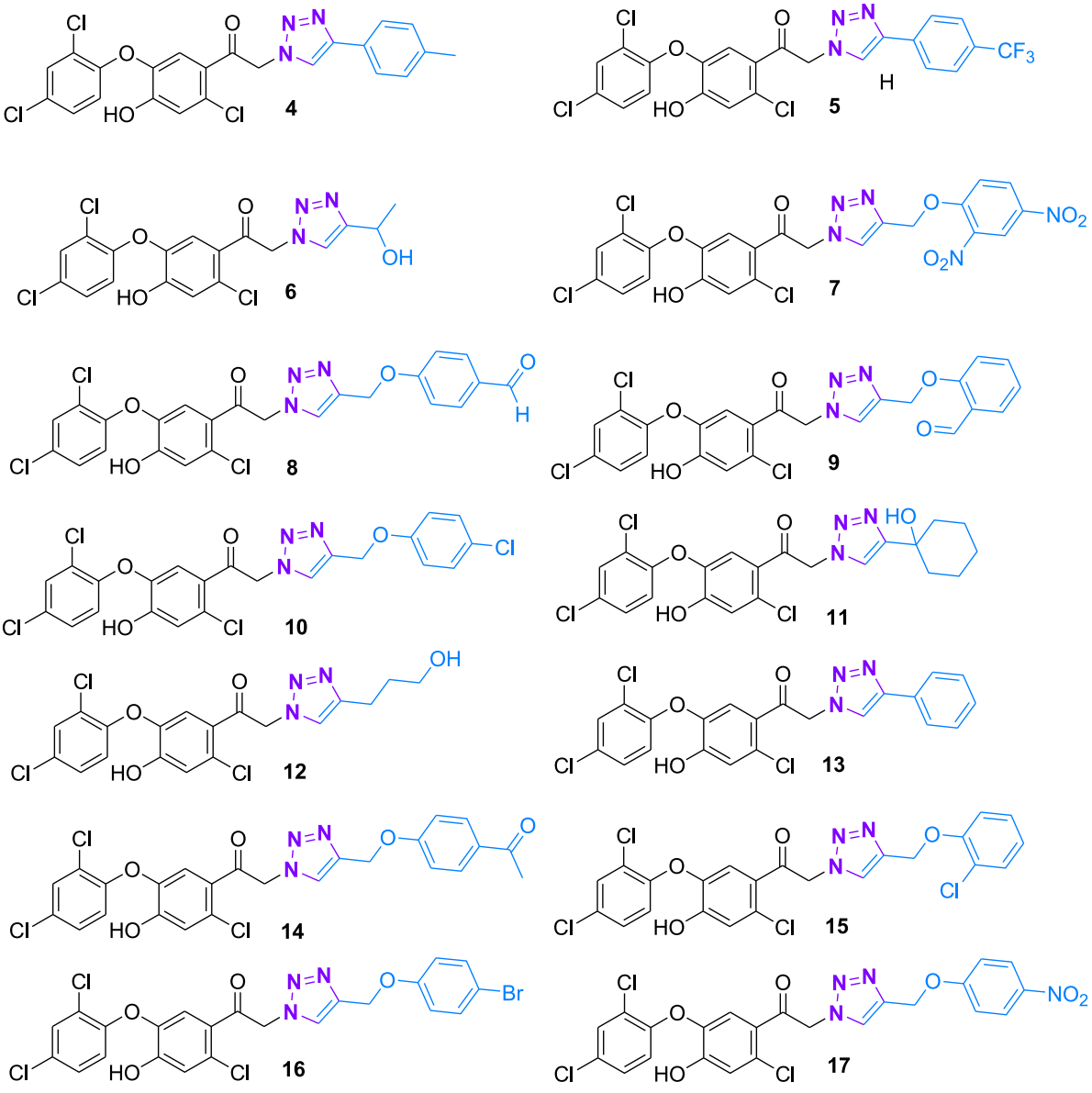

Scheme 2. Structure of 1,2,3-triazoles Difenoconazole analogues **4**–**17**.

2.4.4. Culture conditions

For the tests against bacteria, Mueller Hinton agar was used as culture medium. For tests against *Candida albicans*, Mueller Hinton agar supplemented with 2% glucose and 0.5 μg/ml of methylene blue was used. The tests against filamentous fungi were determined on Sabouraud Agar (glucose 4%) agar.

2.4.5. Growth of the tested microorganisms

All inocula were prepared by resuspension or surface scraping of colonies in 0.1% peptone water (with 0.1% v/v Tween 80 for filamentous fungi) until reaching the desired microbial concentration. The inocula were spread over the entire surface of the agar.

2.4.6. Disk diffusion assay

Bacterial and fungal suspensions were adjusted to a 0.5 McFarland standard corresponding to 1×10^8 CFU/mL. 10 µl of each isolate suspension were inoculated onto three, 5 mm diameter Whatman #1 filter paper disks. Bacterial and yeast cultures were incubated at 37 °C for 24 h. Filamentous fungal cultures were incubated at 25–30 °C for 5 days. Inhibition zones were determined in mm. The Kruskal–Wallis test was used to compare k independent samples. Statistical testing was performed with SPSS software (SPSS Inc., Chicago, Ill.).

2.5. Computational details

All molecules were optimized in the framework of density functional theory (DFT) within the Kohn-Sham formalism (KS). Despite the exact formalism of the KS equations, only approximations of the exchange-correlation potential of the mean-field are known. In here, we use the hybrid functional B3LYP [33] which includes the Becke's three parameter non-local exchange functional [34], with the non-local correlation functional of Lee [35]. Alongside the TZVP [36,37] basis set in the ORCA 4.1.3 [38] and ADF 2014 [39] packages. The Fukui function values [40] were obtained via conceptual DFT as implemented in ADF, as well as the relaxed scan over the dihedral selected with step size of 20°. The ab-initio calculations were done in the package ORCA with the basis set def2-SVP [41], and the RHF level of theory. Non-covalent interactions were extracted with NCIPlot4 at promolecular level of theory [42].

Table 1
Spectroscopic characterization of 1,2,3-triazoles Difenoconazole analogues.

Com-pound	IR (ν_{max}, cm^{-1})	^{1}H NMR (ppm)	^{13}C NMR (ppm)
4	3053, 2921, 2856, 1690, 1594, 1472, 1279, 1229, 1157, 798, 864	7.85 (s, 1H), 7.63 (d, *J* = 8.1 Hz, 2H), 7.36 (d, *J* = 2.6 Hz, 1H), 7.30 (s, 1H), 7.14 (d, *J* = 7.8 Hz, 2H), 7.10 – 7.04 (m, 2H), 6.73 (d, *J* = 8.8 Hz, 1H), 5.80 (s, 2H), 2.29 (s, 3H)	189.3, 153.6, 150.9, 147.4, 142.4, 137.5, 130.0, 129.4, 129.1, 128.6, 127.8, 127.4, 125.3, 125.1, 121.9, 121.2, 119.4, 119.3, 58.1, 20.9
5	3064, 1231, 2000, 1678, 1472, 1279, 1156, 2930, 760, 1324 (C-F), 867	8.05 (d, *J* = 8.0 Hz, 4H), 7.75 (d, *J* = 8.1 Hz, 4H), 7.52 (d, *J* = 2.4 Hz, 1H), 7.46 (d, *J* = 6.5 Hz, 2H), 7.24 (dd, *J* = 8.8, 2.5 Hz, 4H), 6.90 (d, *J* = 8.6 Hz, 2H), 6.00 (s, 4H)	194.1, 158.8, 155.9, 150.9, 147.4, 138.9, 135.0, 132.8, 130.7 – 130.0 (m), 127.8 (d, *J* = 5.1 Hz), 127.0, 124.3 (d, *J* = 19.1 Hz), 82.5.
6	3053, 2921, 2856, 1594, 1472, 1279, 1157, 1229, 1472	10.61 (bs, 1H), 7.57 (s, 1H), 7.41 – 7.32 (m, 1H), 7.10 (dd, *J* = 8.8, 2.6 Hz, 1H), 7.06 (s, 1H), 6.73 (d, *J* = 8.8 Hz, 1H), 5.73 (s, 2H), 4.96 (q, *J* = 6.5 Hz, 1H), 1.48 (d, *J* = 6.5 Hz, 3H)	189.6, 153.7, 152.9, 150.9, 143.2, 130.6, 129.6, 129.5, 128.3, 125.7, 125.7, 122.3, 121.6, 120.2, 119.6, 63.0, 58.5, 23.3
7	3053, 2921, 2856, 1690, 1594, 1471, 1274, 1229, 1157, 798, 864	9.15 (s, 1H), 8.53 (d, *J* = 8.1 Hz, 2H), 7.46 (d, *J* = 2.6 Hz, 1H), 7.43 (s, 1H), 7.14 (d, *J* = 7.8 Hz, 2H), 7.10 – 7.04 (m, 2H), 6.73 (d, *J* = 8.8 Hz, 1H), 5.80 (s, 2H), 5.39 (s, 2H)	183.9, 159.3, 150.9, 147.4, 142.4, 137.5, 130.0, 129.4, 129.8, 128.6, 127.8, 127.4, 125.3, 125.1, 121.9, 121.2, 119.4, 119.3, 58.1, 51.5
8	3105, 2938, 2847, 1714, 1693, 1594, 1476, 1254	9.88 (s, 1H), 8.19 (s, 1H), 7.88 (d, *J* = 8.8 Hz, 2H), 7.83 (s, 1H), 7.72 (d, *J* = 2.6 Hz, 1H), 7.34 (dd, *J* = 8.9, 2.6 Hz, 1H), 7.26 (d, *J* = 8.7 Hz, 2H), 7.15 (s, 1H), 6.83 (d, *J* = 8.9 Hz, 1H), 6.03 (s, 2H), 5.32 (s, 2H)	191.3, 190.2, 163.0, 153.7, 151.8, 141.9, 140.5, 131.8, 129.9, 129.8, 129.4, 128.4, 126.9, 126.5, 124.6, 124.4, 123.1, 119.6, 117.9, 115.2, 61.4, 57.4
9	3160, 3074, 2926, 2876, 1702, 1678, 1596, 1476, 1379, 1279, 1188, 758	10.34 (s, 1H), 8.23 (s, 1H), 7.83 (s, 1H), 7.69 (m, 3H), 7.72 –7.67 (d, *J* = 8.2 Hz, 1H), 7.34 (dd, *J* = 8.8, 2.0 Hz, 1H), 7.15 (s, 1H), 7.11 (t, *J* = 7.5 Hz, 1H), 6.82 (d, *J* = 8.8 Hz, 1H), 6.03 (s, 2H), 5.39 (s, 2H)	190.2, 189.1, 189.1, 160.4, 153.8, 151.8, 142.2, 140.5, 136.3, 129.8, 129.4, 128.3, 127.7, 126.9, 126.2, 124.5, 124.5, 124.4, 123.1, 121.1, 119.6, 117.9, 114.2, 62.9, 57.4
10	3057, 2925, 1711, 1664, 1596, 1492, 1474, 1280, 1159, 774	8.15 (s, 1H), 7.84 (s, 1H), 7.73 (d, *J* = 2.5 Hz, 1H), 7.34 (dd, *J* = 8.9, 1.5 Hz, 3H), 7.16 (s, 1H), 7.09 (dd, *J* = 9.0, 2.4 Hz, 2H), 6.83 (d, *J* = 8.9 Hz, 1H), 6.03 (s, 2H), 5.18 (s, 2H)	190.2, 156.9, 153.6, 151.8, 142.3, 140.5, 129.8, 129.4, 129.2, 128.3, 126.9, 126.2, 124.65, 124.54, 124.38, 123.06, 119.4, 117.9, 116.5, 61.3, 57.3
11	3167, 3089, 2932, 2857, 1708, 1601, 1576, 1499, 1474, 1268, 1192, 739	7.82 (s, 1H), 7.79 (s, 1H), 7.73 (d, *J* = 2.0 Hz, 1H), 7.34 (dd, *J* = 8.8, 2.2 Hz, 1H), 7.15 (s, 1H), 6.82 (d, *J* = 8.9 Hz, 1H), 5.93 (s, 2H), 4.89 (bs, 1H), 1.87 (t, *J* = 10.6 Hz, 2H), 1.75 – 1.58 (m, 4H), 1.51 (s, 1H), 1.47 – 1.34 (m, 2H), 1.32 – 1.25 (m, 1H)	190.6, 153.5, 151.8, 140.5, 129.9, 129.9, 129.8, 129.3, 128.6, 128.5, 128.4, 127.3, 126.86, 124.90, 124.25, 123.05, 122.5, 119.5, 119.3, 119.1, 118.9, 117.9, 68.0, 57.1, 37.8, 25.2, 25.2, 21.6, 21.6
12	3150, 3098, 3030, 2967, 2942, 2752, 1737, 1707, 1602, 1556, 1474, 1276	7.81 (s, 1H), 7.75 (s, 1H), 7.73 (d, *J* = 2.5 Hz, 1H), 7.34 (dd, *J* = 9.0, 2.5 Hz, 1H), 7.15 (s, 1H), 6.82 (d, *J* = 8.9 Hz, 1H), 5.92 (s, 2H), 3.44 (t, *J* = 6.3 Hz, 2H), 2.67 (t, *J* = 7.6 Hz, 2H), 1.75 (q, *J* = 6.7 Hz, 2H)	190.5, 153.4, 151.7, 146.6, 140.5, 129.8, 129.3, 128.3, 126.9, 124.8, 124.2, 123.3, 123.1, 119.5, 117.9, 60.0, 57.12, 32.3, 21.6
13	3105, 2934, 1720, 1671, 1660, 1599, 1471, 1287	10.60 (bs, 1H), 7.95 (s, 1H), 7.83 (d, *J* = 7.4 Hz, 2H), 7.51 – 7.28 (m, 5H), 7.17 (d, *J* = 6.5 Hz, 2H), 6.82 (d, *J* = 8.7 Hz, 1H), 5.89 (s, 2H)	189.4, 153.8, 150.9, 147.6, 142.8, 130.4, 130.3, 129.5, 128.9, 128.7, 128.0, 125.8, 125.6, 125.3, 125.2, 121.9, 121.7, 119.7, 119.5, 58.3
14	3105, 2934, 1720, 1660, 1599, 1471,1282	8.18 (s, 1H), 8.00 – 7.89 (m, 2H), 7.83 (s, 1H), 7.72 (d, *J* = 2.5 Hz, 1H), 7.34 (dd, *J* = 8.9, 2.6 Hz, 1H), 7.17 (dd, *J* = 6.6, 2.3 Hz, 3H), 6.83 (d, *J* = 8.9 Hz, 1H), 6.03 (s, 2H), 5.29 (s, 2H), 2.52 (s, 3H)	196.3, 190.2, 161.9, 153.7, 151.8, 142.1, 140.5, 130.5, 130.1, 129.8, 129.4, 128.4, 126.9, 126.4, 124.7, 124.4, 123.1, 119.6, 117.9, 114.5, 61.3, 57.4, 26.4
15	3154, 3069, 2917, 1696, 1667, 1590, 1474, 1279	8.17 (s, 1H), 7.82 (s, 1H), 7.71 (d, *J* = 2.2 Hz, 1H), 7.50 – 7.24 (m, 4H), 7.15 (s, 1H), 6.97 (t, *J* = 7.5 Hz, 1H), 6.82 (d, *J* = 8.8 Hz, 1H), 6.03 (s, 2H), 5.28 (s, 2H)	190.2, 153.7, 153.4, 151.8, 142.2, 140.6, 130.0, 129.8, 129.5, 128.4, 128.3, 126.9, 126.3, 124.7, 124.4, 123.1, 121.9, 121.4, 119.6, 118.0, 114.4, 62.0, 57.4
16	3068, 2918, 2724, 1712, 1664, 1594, 1474, 1379, 1278	8.14 (s, 1H), 7.82 (s, 1H), 7.72 (d, *J* = 2.5 Hz, 1H), 7.54 – 7.41 (m, 2H), 7.34 (dd, *J* = 8.9, 2.5 Hz, 1H), 7.15 (s, 1H), 7.10 – 6.97 (m, 2H), 6.83 (d, *J* = 8.9 Hz, 1H), 6.02 (s, 2H), 5.18 (s, 2H)	190.2, 157.4, 153.7, 151.8, 142.3, 140.6, 132.2, 129.8, 129.5, 128.4, 126.9, 126.3, 124.6, 124.4, 123.1, 119.6, 118.0, 117.1, 112.3, 61.3, 57.4
17	3084, 2926, 1713, 1689, 1592, 1471, 1270	11.39 (bs, 1H), 8.29 – 8.15 (m, 3H), 7.84 (s, 1H), 7.72 (d, *J* = 1.5 Hz, 1H), 7.34 (dd, *J* = 8.5, 2 Hz, 1H), 7.29 (d, *J* = 9 Hz, 2H), 7.16 (s, 1H), 6.83 (d, *J* = 8.9 Hz, 1H), 6.04 (s, 2H), 5.36 (s, 2H)	190.1, 163.3, 153.6, 151.7, 141.6, 141.0, 140.5, 129.8, 129.4, 128.3, 126.9, 126.6, 125.8, 124.6, 124.4, 123.1, 119.6, 117.9, 115.3, 61.9, 57.4

3. Results and discussion

3.1. Chemistry

Target triazoles **4**–**17** analogues to Difenoconazole were prepared from a two-step synthetic route depicted in Scheme 3. The chloroketone intermediate **3** was obtained from a Friedel-Crafts acylation on triclosan with chloroacetyl chloride in 60% yield. The synthesis of the respective dichlorophenoxy phenacyl triazoles **2** was achieved through a one-pot procedure by a consecutive azide substitution - CuAAC reaction in 20–96% yields. These results are summarized in Table 2, showing yields in the last CuAAC reaction step.

All 1,2,3-triazoles Difenoconazole analogues were fully characterized by the conventional spectroscopic techniques, and some selected spectral data of triazoles **4–17** are presented in Table 3 confirming the presence of 1,2,3-triazole ring. For example, IR spectra of triazoles **4**–**17** exhibit an important aromatic N=N stretching vibration band at 1470 cm^{-1} as well as an absorption band ranged from 1270 to 1300 cm^{-1} associated to a cyclic –N–N=N– configuration present in 1,2,3-triazole core according to previous observations described by our group [43].

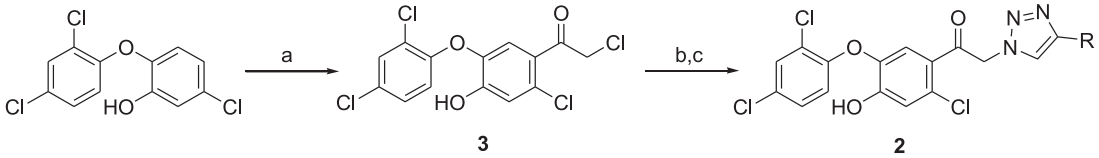

Scheme 3. Reagents and conditions: (a) $ClCH_2COCl$, $AlCl_3$, 1,2-dichloroethane, 0 °C to 65 °C. (b) NaN_3, tBuOH–H_2O, 5 h, 65 °C. (c) Alkyne, $CuSO_4$, ascorbic acid, $NaHCO_3$, R.T.

Table 2
Synthesis of 1,2,3-triazole Difenoconazole analogues.

Compound	R	% Yield
4	4-$CH_3C_6H_4$	40
5	4-$CF_3C_6H_4$	36
6	$CH(OH)CH_3$	45
7	$CH_2O(2,4\text{-}NO_2)C_6H_3$	20
8	$CH_2O(4\text{-}CHO)C_6H_4$	79
9	$CH_2O(2\text{-}CHO)C_6H_4$	72
10	$CH_2O(4\text{-}Cl)C_6H_4$	69
11	$C(OH)(CH_2CH_2)_2\ CH_2$	92
12	$CH_2CH_2CH_2OH$	67
13	Ph	50
14	$CH_2O(4\text{-}COCH_3)C_6H_4$	67
15	$CH_2O(2\text{-}Cl)C_6H_4$	96
16	$CH_2O(4\text{-}Br)C_6H_4$	53
17	$CH_2O(4\text{-}NO_2)C_6H_4$	52

Table 3
Selected spectral data of 4-(1,2,3-triazol-1-yl) salicylic acid derivatives.

Compound	IR (ν_{max}, cm^{-1})		^1H NMR (ppm)		^{13}C NMR (ppm)	
	C=O	$N{=}N_{arom}$	–N–N=N–	Triazole C5-H	C4	C5
4	1690	1472	1279	7.85	147.4	119.2
5	1691	1472	1279	7.57	143.2	119.7
6	1690	1472	1279	7.43	147.4	119.7
7	1693	1471	1274	7.83	151.7	119.2
8	1693	1476	1254	7.86	141.9	119.6
9	1678	1476	1279	7.83	142.9	119.6
10	1669	1474	1280	8.15	142.3	119.6
11	1708	1474	1268	7.79	140.5	119.3
12	1707	1474	1276	7.81	146.6	119.5
13	1671	1471	1287	7.51	147.6	119.5
14	1720	1471	1282	7.83	142.6	119.6
15	1696	1474	1279	7.82	142.2	119.6
16	1712	1474	1278	7.82	142.3	119.6
17	1689	1471	1270	7.84	141.6	119.6

As also mentioned by our group [43], the presence of 1,2,3-triazole ring in compounds **4**–**17** was entirely confirmed through the NMR spectra analysis. A typical singlet signal at 7.51–8.15 ppm is detected in ^1H NMR spectra of compounds **4**–**17** which is attributed to hydrogen on triazole C-5. In addition, two carbon signals at 147 and 119 ppm assigned to triazole C-4 and C-5 are observed in the respective ^{13}C NMR spectra. Some selected spectral data of compounds triazoles **4**–**17** are summarized in Table 2.

3.2. Biological evaluation and antimicrobial activity

The antimicrobial activity of compounds **4**–**17** was evaluated against a series of bacterial and fungal cultures which included *S. aureus*, methicillin-resistant *S. aureus* (MRSA), *E. coli, B. subtilis, P. aeruginosa, K. pneumoniae* and *C. albicans*. In general terms, triazoles **4**–**17** exhibit activity against *S. aureus* and 12 compounds from this group show activity against methicillin-resistant S. aureus (MRSA), as well as 8 compounds against *B. subtilis*, whereas only 5 compounds (**6, 10**–**12**, and **17**) show inhibition against *E. coli* strains. Other observed overall trend is that *S. aureus* was more sensitive to synthesized triazoles due to respective inhibition zones (IZ) were the widest as seen in Fig. 1. In contrast, the growth of Gram-negative bacteria *P. aeruginosa* and *K. pneumoniae* was not inhibited by any tested compound, indicating that these microorganisms probably are also resistant to referred compounds.

According to registered diameters of zone of inhibition (DIZ, Table 4), and subsequent Shapiro Wilk statistic test ($p<0.05$), the inhibition data for *S. aureus*, MRSA, *B. subtilis* and *E. coli* present a non-normal distribution with a significance level of 0.05 through a Kruskal Wallis test, agreeing to other similar studies [44–46] and therefore demonstrating the growth inhibition of these pathogens. As mentioned above, inhibition found for *S. aureus* was higher than other assessed microorganisms. In particular, compounds **6** and **12**, bearing a linear alcohol moiety at triazole C-4, displayed a remarkable activity slightly below Gentamicin standard reference antibiotic. On the other hand, compound **11** containing a cyclic alcohol belongs to a second group in drecreasing order of antibacterial activity, together to compounds **10** and **13** with a (*p*-chlorophenoxy)methyl and phenyl groups respectively. Compounds **7, 9** and **14** showed the lowest inhibition against *S. aureus* (Fig. 2).

A noteworthy activity against MRSA cultures by entitled triazoles was observed (Fig. 3). Indeed, activity found in compound **6** (DIZ = 8.2 mm) is comparable to Gentamicin standard (DIZ = 8.3 mm). Moreover, compounds **12** (DIZ = 7.8 mm) and **16**

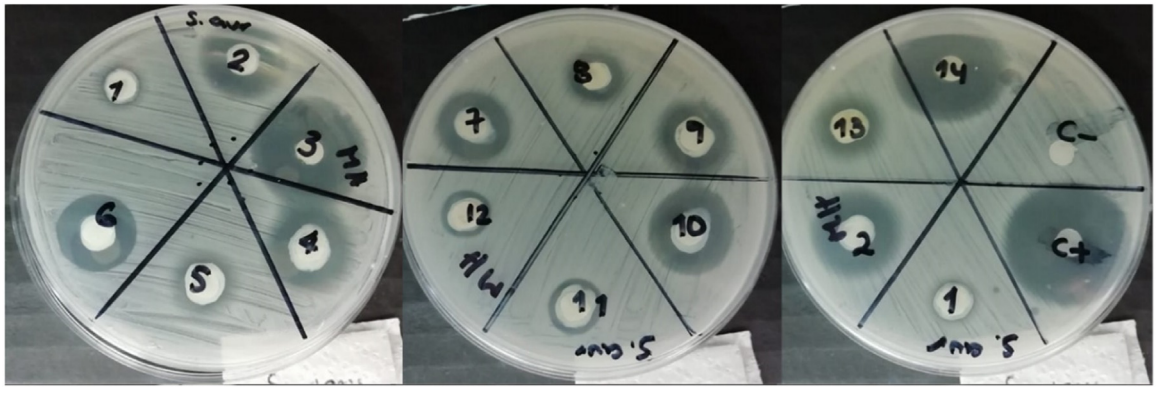

Fig. 1. Diameters of inhibition zones of *S. aureus* culture on inoculation of triazoles **4**–**17**.

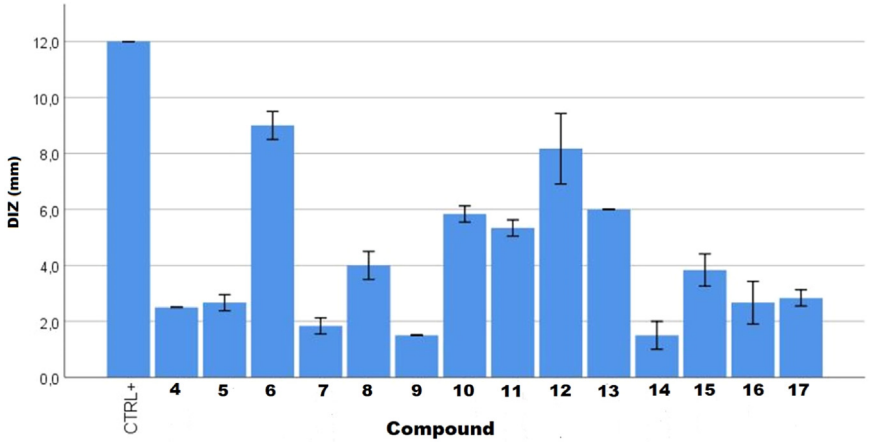

Fig. 2. Diameters of inhibition zones of *S. aureus* culture on inoculation of triazoles **4**–**17**.

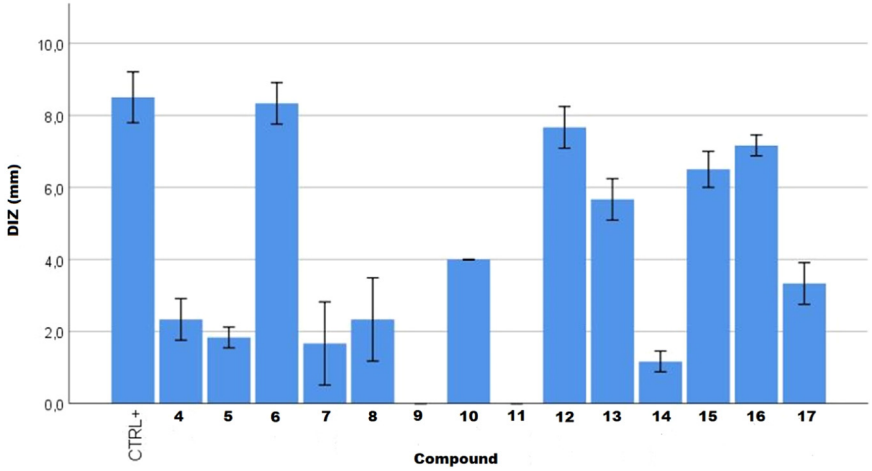

Fig. 3. Diameters of inhibition zones of MRSA culture on inoculation of triazoles **4**–**17**.

Table 4
Values of diameter of the inhibition zone in mm for compounds **4**–**17**.

Compound	Diameter of the Inhibition Zones (mm)			
	S. aureus ATCC 29213	MRSA	*E. coli* ATCC 700891	*C. albicans* ATCC 90028
4	2.5	2.2	–	–
5	2.7	1.9	–	–
6	9	8.2	3.8	–
7	1.8	1.7	–	–
8	4	2.2	–	–
9	1.5	–	–	–
10	5.8	4	3.5	–
11	5.3	–	1.3	–
12	8.2	7.8	2.7	–
13	6	5.8	–	–
14	1.5	1.1	–	–
15	3.8	6.3	–	–
16	2.7	7.2	–	–
17	2.8	3.5	1.3	
Gentamicin	12	8.3	12	–
Fluconazole	–	–	–	15.5

(DIZ = 7.2 mm) also exhibit an important activity against this kind of strains.

Antibacterial activity of triazoles **4**–**17** against *B. subtilis* (Fig. 4) and *E. coli* (Fig. 5) strains resulted lower than those observed for *S. aureus* and MRSA. In this regard, compound **6** is the only compound with the highest activity for the four bacteria that showed inhibition, followed by compound **12** which also resulted active, although in a smaller proportion.

In a similar fashion, antifungal activity was tested on compounds **4**–**17** against strains of *C. albicans, Fusarium sp*. and *A. niger*. While it is true that no significant inhibition was detected, a pigmentation reduction of the mycelium of *Fusarium sp*. was observed (Fig. 6), which hints a kind of inhibition [47,48]. Likewise, sporulation on *A. niger* cultures was affected as seen in Fig. 6. Consequently, further studies are required to verify this activity.

3.3. Computational analysis

For computational analysis purposes, molecules **6, 12, 15** and **16** were selected due to these compounds resulted the most effective against Methicillin-resistant *Staphylococcus aureus* (MRSA) strains. A minimal geometric model was suggested as well as some conformers, based on its electronic energy. In the case of compound **6**, 4-(1–hydroxy)ethyl substituent on triazole moiety was rotated in two minimal positions in combination with the two minimal positions on phenyl OH group. The resulting set of four conformers is aligned based on the most stable one and presented in Fig. 7 and represented with capital A and set as the zero energy for comparison. Thus, subfigure (a) presents relative energies of 0.66 kcal/mol, 3.30 kcal/mol, and 4.66 kcal/mol, for conformers B, C, and D, respectively. The subfigure (b) presents relative energies of 3.12 kcal/mol, 3.24 kcal/mol, and 2.73 kcal/mol for conformers B,

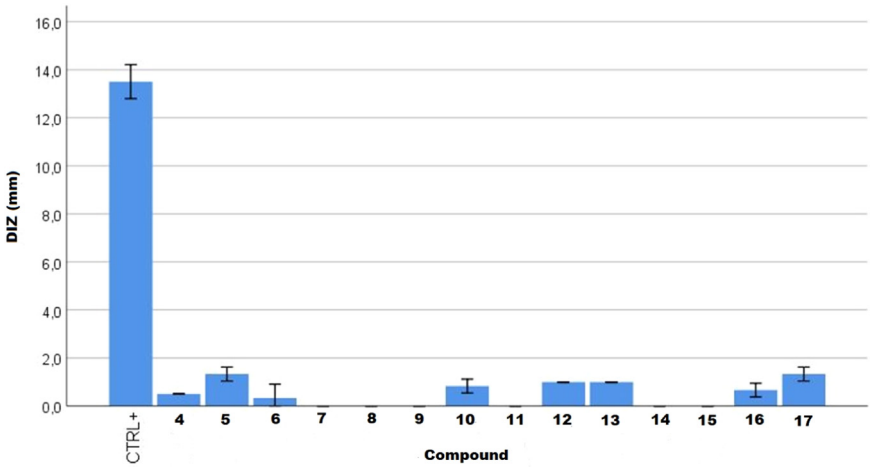

Fig. 4. Diameters of inhibition zones of *B. subtilis* culture on inoculation of triazoles **4**–**17**.

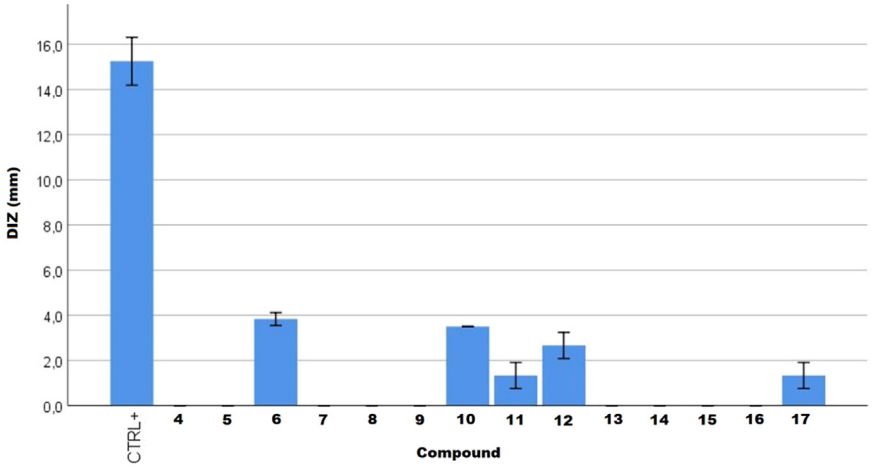

Fig. 5. Diameters of inhibition zones of *E. coli* culture on inoculation of triazoles **4**–**17**.

C, and D, respectively. Showing that the most stable and probable geometrical configuration lies on A representation.

As observed in Fig. 7, the combination of both $CH(OH)CH_3$ and OH groups is pointing out to same direction activating the triazole ring, i.e., the triazole ring shows red zones (nucleophilicity behavior based on Fukui's Function). This behavior is also observed in compound **12**, see Fig. 8. A plausible explanation of this activity lies on the conjugation through non-covalent interactions (NCI, hydrogen bonding) in these molecules. The systems (a) and (b) from compound **12** present a higher activity based on Fukui function

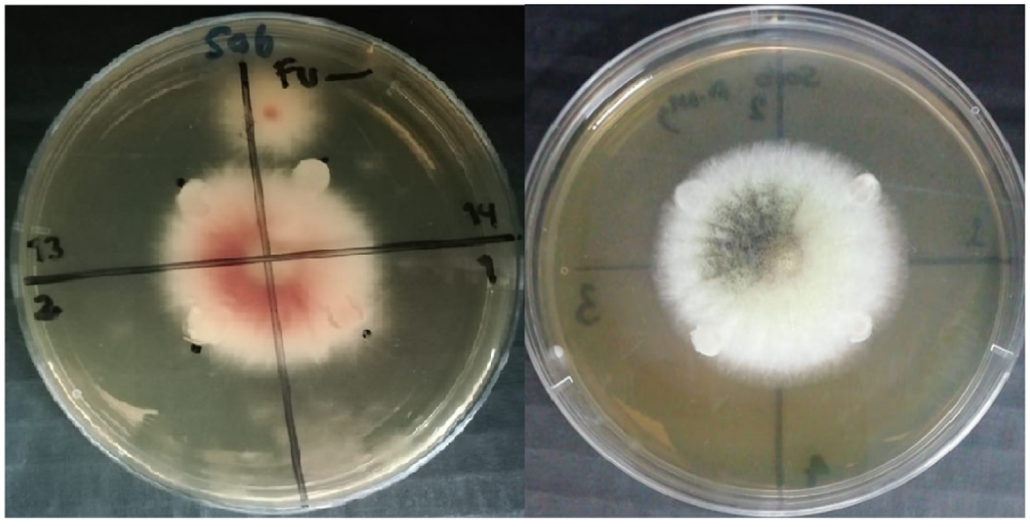

Fig. 6. Left: pigmentation reduction of the mycelium of *Fusarium sp*. Right: sporulation reduction on *A. niger*.

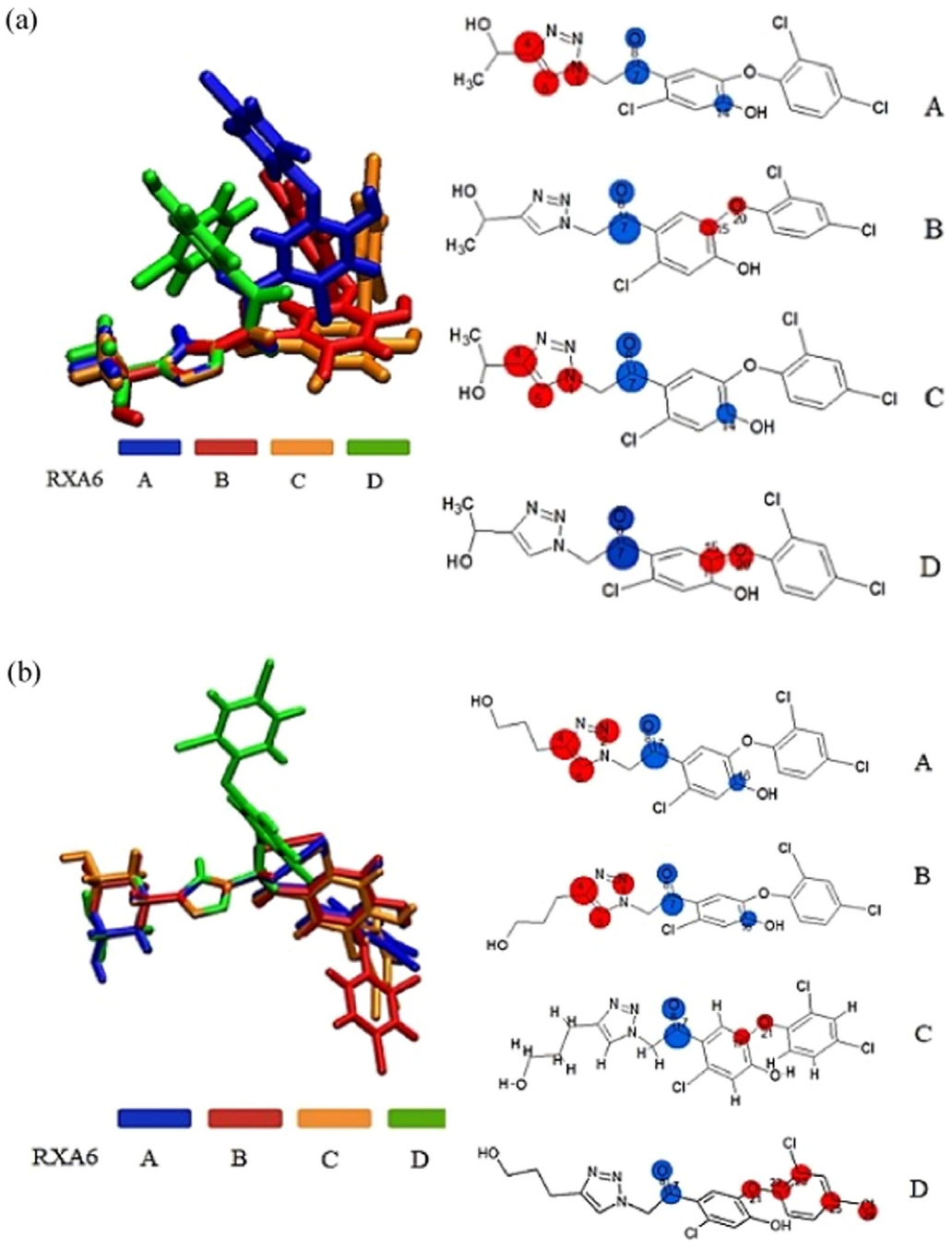

Fig. 7. RMSD and Fukui functions for (a) compound **6** and (b) compound **12**.

over triazole ring. As illustrated in Fig. 8, there is an outer region around aromatic rings with attractive NCI. This lack of interactions in systems (c) and (d) would be responsible of the lack of activity on Fukui function in these triazole conformers. This shed light to a bigger relation between biological activity and the NCI, than biological activity and Fukui's Function.

Furthermore, a relaxed scan over the potential energy surface (PES) was determined, taking into account one dihedral bond of interest. This allows to explore others possible and stable conformers that could exist as local minima and possible geometrical conformation with biological activity. In Fig. 9, a relaxed scan for compound **6** systems is plotted, displaying different stable conformers over the PES, where the most stable is the initial (a) system which can be transformed to (b), whereas relaxed conformers d and c once are converted into S or b.

On the flip side, compounds **15** and **16** have a lack of Fukui function over the triazole as depicted in Fig. 10. This lack of activity suggests that referred molecules might not present a high response against MRSA. Nevertheless, the NCI reveals that weak hydrogen bonds conjugations are still present in both systems (Fig. 11). Thus, the inhibition activity is probably more related to the conjugation of NCI in whole system than Fukui functions as depicted previously.

These elements give rise to infer the importance of a synergistic behavior between the conformational structure and the non-covalent interactions over the Fukui function activity and, in conse-

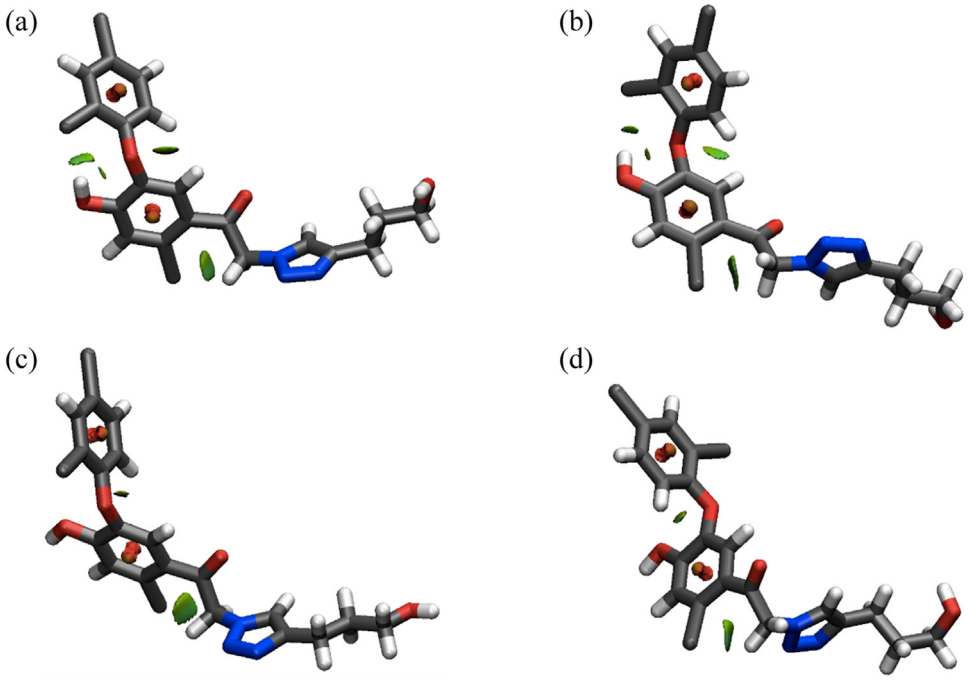

Fig. 8. Non-covalent interactions for different conformers of compound **12**. Green plateau reveals attractive and weak interactions while red ones to steric repulsive interactions.

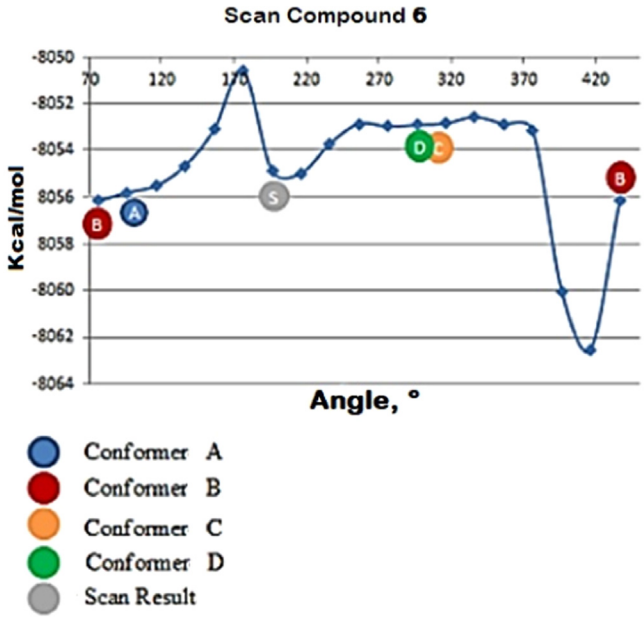

Fig. 9. Relaxed scan for compound **6** system.

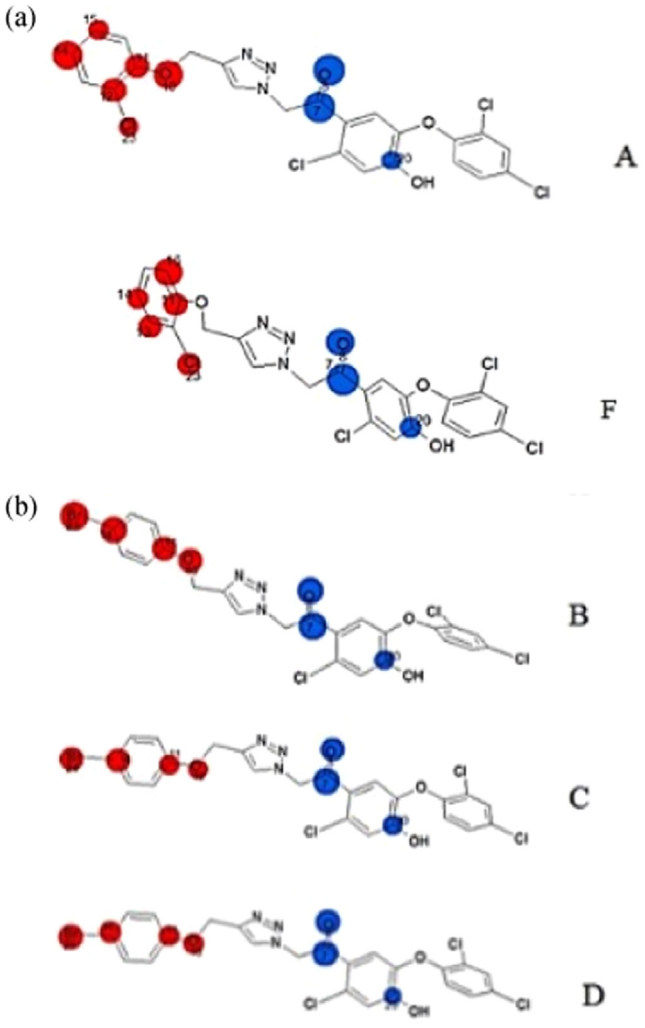

Fig. 10. Fukui functions for (a) compound **15** and (b) compound **16** systems.

quence, antimicrobial activity in these molecules as experimentally observed.

4. Conclusions

In summary, a small library of 1-(2–chloro-5-(2,4-dichlorophenoxy)–4-hydroxyphenyl)–2-(1,2,3-triazolyl)ethan-1-one derivatives analogues to Difenonazole was prepared using the Click Chemistry approach as key reaction through a short synthetic sequence, requiring two steps from commercially available starting materials in yields up 96%. Spectroscopic analysis confirmed the proposed structure for compounds **4**–**17** which were also screened

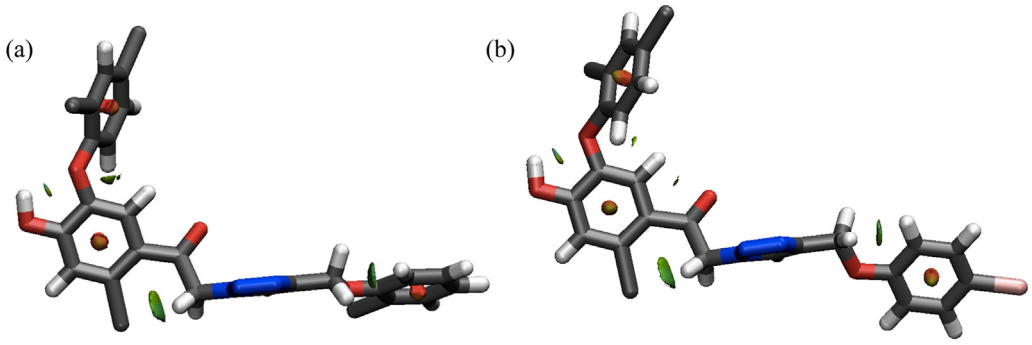

Fig. 11. NCI for selected conformers of (a) compound **15** and (b) compound **16**.

against strains of *S. aureus*, methicillin-resistant *S. aureus* (MRSA), *E. coli, B. subtilis, P. aeruginosa, K. pneumoniae* and *C. albicans*. The antimicrobial activities found in some synthesized compounds hint promising applications as antibacterials, particularly triazole derivatives **6** and **12** with hydroxy alkyl groups substituted at triazole C-4, showed a potential antibacterial activity inhibiting *S. aureus* and MRSA strains, which probably is related to a synergistic behavior between the conformational structure and the non-covalent interactions over the Fukui function activity on triazole ring assisted by the mentioned hydroxy alkyl groups. Based upon the before mentioned observations, these products might be appropriate candidates for further modifications to achieve potent antimicrobial activities, driving to more studies about this topic.

Declaration of Competing Interest

The authors declare that they have no known competing financial interests or personal relationships that could have appeared to influence the work reported in this paper.

CRediT authorship contribution statement

Juana Suárez-García: Methodology, Investigation. **Ma.-Angeles Cano-Herrera:** Methodology, Investigation, Data curation, Validation, Formal analysis, Writing – original draft. **Angela María-Gaviria:** Methodology, Investigation. **Víctor Manuel Osorio-Echeverri:** Methodology, Investigation, Data curation, Formal analysis, Validation, Writing – original draft. **Hugo Mendieta-Zerón:** Methodology, Data curation, Validation. **David Arias-Olivares:** Methodology, Investigation, Data curation, Validation, Software, Writing – original draft. **Julie Benavides-Melo:** Methodology, Investigation, Data curation, Validation, Formal analysis, Software. **Luis Carlos García-Sánchez:** Software, Formal analysis, Supervision, Project administration, Funding acquisition. **Josue García-Ortíz:** Methodology, Investigation, Software. **Andrés Becerra-Buitrago:** Methodology, Investigation, Software. **Jessica Valero-Rojas:** Methodology, Investigation, Software. **Mateo Rodríguez-González:** Methodology, Investigation, Software. **Marco Antonio García-Eleno:** Validation, Formal analysis, Data curation. **Erick Cuevas-Yañez:** Conceptualization, Investigation, Validation, Supervision, Project administration, Funding acquisition, Writing – original draft, Writing – review & editing.

Data Availability

Data will be made available on request.

Acknowledgments

Financial support from CONACYT (Project No. A1-S-18230 and fellowships for J. S. G., CVU: 388438 and M. A. C. H., CVU: 173992), as well as Centro de Investigaciones y Desarrollo Científico (CIDC)-Universidad Distrital Francisco José de Caldas, project No. 4-50-598-19 and CECAD for the Computing Facility are gratefully acknowledged. The authors would like to N. Zavala, A. Nuñez, L. Triana and M. C. Martínez for the technical support.

Supplementary materials

Supplementary material associated with this article can be found, in the online version, at doi:10.1016/j.molstruc.2023.135053.

References

[1] C. Lass-Flörl, Triazole antifungal agents in invasive fungal infections: a comparative review, Drugs 71 (2011) 2405–2419.
[2] L.N. Jefreys, H. Poddar, M. Golovanova, C.W. Levy, H.M. Girvan, K.J. McLean, M.W. Voice, D. Leys, A.W. Munro, Novel insights into P450 BM3 interactions with FDA-approved antifungal azole drugs, Sci. Rep.-UK 9 (2019) 1577.
[3] J. Ruegg, Biology and control of *Entyloma eryngii* (Cda.) de by., the cause of a leaf spot disease on the blue thistle (*Eryngium alpinum L.*), J. Phytopathol. 130 (1990) 9–16.
[4] T.R. Roberts, D.H. Hutson, P.J. Jewess, P.W. Lee, P.H. Nicholls, J.R. Plimmer, in: Metabolic Pathways of Agrochemicals, Part 2: Insecticides and Fungicides, Royal Society of Chemistry, Cambridge, 1999, p. 1036.
[5] F. Dong, J. Li, B. Chankvetadze, Y. Cheng, J. Xu, X. Liu, Y. Li, X. Chen, C. Bertucci, D. Tedesco, R. Zanasi, Y. Zheng, Chiral triazole fungicide difenoconazole: absolute stereochemistry, stereoselective bioactivity, aquatic toxicity, and environmental behavior in vegetables and soil, Environ. Sci. Technol. 47 (2013) 3386–3394.
[6] H. Wang, Y. Huang, J. Wang, X. Chen, K. Wei, M. Wang, S. Shang, Activities of azoxystrobin and difenoconazole against *Alternaria alternata* and their control efficacy, Crop Prot 90 (2016) 54–58.
[7] M. Reuveni, D. Sheglov, N. Sheglov, R. Ben-Arie, D. Prusky, Sensitivity of Red Delicious apple fruit at various phenologic stages to infection by Alternaria alternata and moldy-core control, Eur. J. Plant Pathol. 108 (2002) 421–427.
[8] D. Shtienberg, J. Dreishpoun, Suppression of Alternaria leaf spot in Pima cotton by systemic fungicides, Crop Prot 10 (1991) 381–385.
[9] G.P. Munkvold, J.K. O'Mara, Laboratory and growth chamber evaluation of fungicidal seed treatments for maize seedling blight caused by fusarium species, Plant Dis 86 (2002) 143–150.
[10] K.W. Jayasena, R. Loughman, J. Majewski, Evaluation of fungicides in control of spot-type net blotchon barley, Crop Prot. 21 (2002) 63–69.
[11] R.J. Cook, A.Y. El-Banna, D. Vakoch, H. Zhang, Yield responses of direct-seeded wheat to rhizobacteria and fungicide seed treatments, Plant Dis. 86 (2002) 780–784.
[12] H. Dahmen, T. Staub, Protective, curative, and eradicant activity of difenoconazole against *Venturia inaequalis, Cercospora arachidicola* and *Alternaria solani*, Plant Dis. 76 (1992) 774–777.
[13] P. Bowyer, D.W. Denning, Environmental fungicides and triazole resistance in Aspergillus, Pestic. Manag. Sci. 70 (2014) 173–178.
[14] E. Snelders, S.M.T. Camps, A. Karawajczyk, G. Schaftenaar, G.H.J. Kema, H.A. van der Lee, C.H. Klaassen, W.J.G. Melchers, P.E. Verweij, Triazole Fungicides Can Induce Cross-Resistance to Medical Triazoles in *Aspergillus fumigatus*, PLoS ONE 7 (2012) e31801.
[15] S.J. Howard, D. Cerar, M.J. Anderson, A. Albarrag, M.C. Fisher, A.C. Pasqualotto, M. Laverdiere, M.C. Arendrup, D.S. Perlin, D.W. Denning, Frequency and evolution of azole resistance in aspergillus fumigatus associated with treatment failure, Emerg. Infect. Dis. 15 (2009) 1068–1076.
[16] S. Kunz, H. Deising, K. Mendgen, Acquisition of resistance to sterol demethylation inhibitors by populations of *Venturia inaequalis*, Phytopathology 87 (1997) 1272–1278.

[17] J.P.F. D'Mello, A.M.C. Macdonald, D. Postel, W.T.P. Dijksma, A. Dujardin, C.M. Placinta, Pesticide use and mycotoxin production in *Fusarium* and *Aspergillus* phytopathogens, Eur. J. Plant Pathol. 104 (1998) 741–751.
[18] J. Suárez-García, M.A. Cano-Herrera, A. Ramírez-Villalva, A. Fuentes-Benites, N. Zavala-Segovia, M.A. García-Eleno, M.V.B. Unnamatla, E. Cuevas-Yañez, Synthesis and antifungal activity evaluation of 1-(2-benzyloxy-2-phenylethyl)-1,2,3-triazole miconazole analogs, Pharm. Chem. J. 55 (2021) 436–440.
[19] A. Zambrano-Huerta, D.D. Cifuentes-Castañeda, J. Bautista-Renedo, H. Mendieta-Zerón, R.C. Melgar-Fernández, S. Pavón-Romero, M. Morales-Rodríguez, B.A. Frontana-Uribe, N. González-Rivas, E. Cuevas-Yañez, Synthesis and in vitro biological evaluation of 1,3-bis-(1,2,3-triazol-1-yl)-propan-2-ol derivatives as antifungal compounds fluconazole analogues, Med. Chem. Res. 28 (2019) 571–579.
[20] M. Haroun, C. Tratrat, H. Kochkar, A.B. Nair, Recent advances in the development of 1,2,3-triazole-containing derivatives as potential antifungal agents and inhibitors of lanosterol 14α-demethylase, Curr. Top. Med. Chem. 21 (2021) 462–506.
[21] A.K. Estrada-Valdés, E. Cuevas-Yañez, Design and synthesis of antifungal compounds from 1,2,3-triazoles through the click chemistry approach, Org. Med. Chem. Int. J. 8 (2019) 555734.
[22] K. Bozorova, J. Zhao, H.A. Aisa, 1,2,3-Triazole-containing hybrids as leads in medicinal chemistry: a recent overview, Bioorg. Med. Chem. 27 (2019) 3511–3531.
[23] E. Bonandi, M.S. Christodoulou, G. Fumagalli, D. Perdicchia, G. Rastelli, D. Passarella, The 1,2,3-triazole ring as a bioisostere in medicinal chemistry, Drug Discov. Today 22 (2017) 1572–1581.
[24] P. Thirumurugan, D. Matosiuk, K. Jozwiak, Click chemistry for drug development and diverse chemical-biology applications, Chem. Rev. 113 (2013) 4905–4979.
[25] C.H. Zhou, Y. Wang, Recent researches in triazole compounds as medicinal drugs, Curr. Med. Chem. 19 (2012) 239–280.
[26] S.G. Agalave, S.R. Maujan, V.S. Pore, Click Chemistry: 1,2,3-Triazoles as Pharmacophores, Chem. Asian J. 6 (2011) 2696–2718.
[27] R.D. Jones, H.B. Jampani, J.L. Newman, A.S. Lee, Triclosan: a review of effectiveness and safety in health care settings, Am. J. Infect. Control 28 (2000) 184–196.
[28] C.W. Levy, A. Roujeinikova, S. Sedelnikova, P.J. Baker, A.R. Stuitje, A.R. Slabas, D.W. Rice, J.B. Rafferty, Molecular basis of triclosan activity, Nature 398 (1999) 383–384.
[29] A.A.S. Ali, D. Khan, A. Naqvi, F.F. Al-blewi, N. Rezki, M.R. Aouad, M. Hagar, Design, synthesis, molecular modeling, anticancer studies, and density functional theory calculations of 4–(1,2,4-triazol-3-ylsulfanylmethyl)-1,2,3-triazole derivatives, ACS Omega 6 (2021) 301–316.
[30] M. Fizer, M. Slivka, N. Korol, O. Fizer, Identifying and explaining the regioselectivity of alkylation of 1,2,4-triazole-3-thiones using NMR, GIAO and DFT methods, J. Mol. Struct. 1223 (2021) 128973.
[31] P.P. Zamora, K. Bieger, A. Cuchillo, A. Telloa, J.P. Muena, Theoretical determination of a reaction intermediate: Fukui function analysis, dual reactivity descriptor and activation energy, J. Mol. Struct. 1227 (2021) 129369.
[32] National Committee Clinical Laboratory StandardsPerformance Standards for Antimicrobial Disk Susceptibility Tests; M100-S21, Clinical and Laboratory Standards Institute, Wayne, PA, USA, 2011 Volume 31.
[33] P.J. Stephens, F.J. Devlin, C.F. Chabalowski, M.J. Frisch, Ab initio calculation of vibrational absorption and circular dichroism spectra using density functional force fields, J. Phys. Chem. 98 (1994) 11623–11627.
[34] A.D. Becke, Density-functional thermochemistry. III. The role of exact exchange, J. Chem. Phys. 98 (1993) 5648–5652.
[35] C. Lee, W. Yang, R.G. Parr, Development of the Colle-Salvetti correlation-energy formula into a functional of the electron density, Phys. Rev. B 37 (1988) 785–789.
[36] A. Schaefer, H. Horn, R. Ahlrichs, Fully optimized contracted Gaussian-basis sets for atoms Li to Kr, J. Chem. Phys. 97 (1992) 2571–2577.
[37] A. Schaefer, C. Huber, R. Ahlrichs, Fully optimized contracted Gaussian-basis sets of triple zeta valence quality for atoms Li to Kr, J. Chem. Phys. 100 (1994) 5829–5835.
[38] F. Neese, F. Wennmohs, U. Becker, C. Riplinger, The ORCA quantum chemistry program package, J. Chem. Phys. 152 (2020) 224108.
[39] G. te Velde, F.M. Bickelhaupt, E.J. Baerends, C. Fonseca-Guerra, S.J.A. van Gisbergen, J.G. Snijders, T. Ziegler, Chemistry with ADF, J. Comput. Chem. 22 (2001) 931–967.
[40] P. Fuentealba, On the condensed Fukui function, J. Chem. Phys. 113 (2000) 2544.
[41] F. Weigend, R. Ahlrichs, Balanced basis sets of split valence, triple zeta valence and quadruple zeta valence quality for H to Rn: design and assessment of accuracy, Phys. Chem. Chem. Phys. 7 (2005) 3297–3305.
[42] R. Laplaza, F. Peccati, D. Arias-Olivares, J. Contreras-García, Visualizing non–covalent interactions with NCIPLOT, in: S. Grabowsky (Ed.), Complementary Bonding Analysis, Walter de Gruyter GmbH, Berlin, 2021, p. 353.
[43] Z.G. Ríos-Malváez, M.A. Cano-Herrera, J.C. Dávila-Becerril, G. Mondragón–Solórzano, M.T. Ramírez-Apan, D. Morales-Morales, J. Barroso-Flores, J.G. Santillán-Benítez, M.V.B. Unnamatla, M.A. García-Eleno, N. González-Rivas, E. Cuevas-Yañez, Synthesis, characterization and cytotoxic activity evaluation of 4-(1,2,3-triazol-1-yl) salicylic acid derivatives, J. Mol. Struct. 1225 (2021) 129149.
[44] E. Bodrumlu, T. Alaçam, Evaluation of antimicrobial and antifungal effects of iodoform-integrating Gutta-Percha, J. Can. Dent. Assoc. 72 (2006) 733.
[45] N.H. Mahdally, R.F. George, M.T. Kashef, M. Al-Ghobashy, F.E. Murad, A.S. Attia, Staquorsin: a novel staphylococcus aureus Agr-mediated quorum sensing inhibitor impairing virulence in vivo without notable resistance development, Front. Microbiol. 12 (2021) 700494.
[46] S. Kesici, M. Demirci, U. Kesici, Antimicrobial effects of fentanyl and bupivacaine: an in vitro study, Rev. Bras. Anestesiol. 70 (2020) 357–363.
[47] T. Schöneberg, K. Kibler, M. Sulyok, T. Musa, T.D. Bucheli, F. Mascher, M. Bertossa, R.T. Voegele, S. Vogelgsang, Can plant phenolic compounds reduce Fusarium growth and mycotoxin production in cereals? Food Addit. Contam. A 35 (2018) 2455–2470.
[48] E. Gnonlonfoun, G. Fotin, A. Risler, A. Elfassy, S. Schwebel, M. Schmitt, F. Borges, C. Mangavel, A.M. Revol-Junelles, M. Fick, X. Framboisier, E. Rondags, Inhibition of the growth of fusarium tricinctum and reduction of its enniatin production by erwinia gerundensis isolated from Barley Kernels, J. Am. Soc. Brew. Chem. (2022), doi:10.1080/03610470.2022.2041970.